3110 *Chem. Mater.* **2009,** *21,* 3110–3116
DOI:10.1021/cm900244g

CHEMISTRY OF MATERIALS
Article

# Nanotubular Mesoporous PdCu Bimetallic Electrocatalysts toward Oxygen Reduction Reaction

Caixia Xu,[†,‡] Yan Zhang,[‡] Liqin Wang,[‡] Liqiang Xu,[‡] Xiufang Bian,[†] Houyi Ma,*[,‡] and Yi Ding*[,†,‡]

[†]*Key Laboratory of Liquid Structure and Heredity of Materials, Ministry of Education, Shandong University, Jinan 250061, China, and* [‡]*School of Chemistry and Chemical Engineering, Shandong University, Jinan 250100, China*

*Received January 27, 2009. Revised Manuscript Received June 12, 2009*

We describe the fabrication of novel PdCu bimetallic nanocomposites with hierarchically hollow structures through a simple galvanic replacement reaction using dealloyed nanoporous copper (NPC) as both a template and reducing agent. The reaction process was monitored by UV−vis absorbance spectra and X-ray diffraction (XRD), which clearly demonstrate a structure evolution from NPC precursor to a Pd-rich PdCu alloy structure upon the completion of the reaction. Structure characterization by means of transmission electron microscope (TEM) and scanning electron microscope (SEM) indicates that the replacement reaction between NPC and $[PdCl_4]^{2-}$ solution results in a nanotubular mesoporous structure with a nanoporous shell, which is comprised of interconnected alloy nanoparticles with size around 3 nm. The resulted PdCu nanostructure shows superior activity toward oxygen reduction reaction (ORR) with a half-wave potential at 0.840 V, which is significantly better than that of the commercial Pt/C catalyst.

## Introduction

Pt-based electrocatalysts are currently the most employed cathode catalysts in proton-exchange membrane fuel cells (PEMFCs) due to their high activity toward oxygen reduction reaction (ORR).[1,2] However, the high cost and low durability of Pt-based catalysts pose a severe challenge to the commercialization of PEMFCs.[3] Now, great efforts have been devoted to seeking for alternative nonplatinum catalysts with low cost and high ORR activity.[4,5] Among them, Pd nanostructures have stimulated considerable attention recently because they were found to exhibit unique catalytic activities toward ORR especially when they are combined with certain transition metals.[6−10] For instance, Adzic and co-workers have observed higher ORR activity from Pd−Fe alloy nanoparticles as compared with Pt/C catalyst.[6] Fernandez et al. found that unique ORR activity can be achieved on Pd−Ti and Pd−Co−Au alloy nanoparticles.[7] Wang et al. recently found that carbon-supported Pd−Cu alloy catalysts offer a greatly enhanced ORR activity compared to the monometallic Pd electrocatalyst.[11] In addition, similar ORR activity was also observed on sputtered Pd−Co films, Co modified Pd/C nanoparticles, and so forth.[8,10]

Hollow metallic nanostructures represent a class of interesting materials with high surface area, low density, and rich surface chemistry to allow function integration.[12] The in situ galvanic replacement reaction based on sacrificial Ag nanoparticle templates, a method recently developed by Xia and co-workers, has been a very effective route to prepare hollow Au, Pt, and Pd nanostructures.[13−16] This method has been further developed by several research groups by, for example,

*Corresponding author. Y.D.: e-mail, yding@sdu.edu.cn; phone, +86-531-88366513; fax, +86-531-88366280. H.M.: e-mail, hyma@sdu.edu.cn; phone, +86-531-88364959; fax, +86-531-88564464.

(1) Tarasevich, M. R.; Sadkowski, A.; Yeager, E. In Comprehensive Treatise of Electrochemistry; Conway, B. E., Bockris, J. O. M., Yeager, E., Khan, S. U. M., White, R. E., Eds.; Plenum Press: New York, 1983; Vol. 7, p 301.
(2) Markovic, N. M.; Ross, P. N. *Electrochim. Acta* **2000**, *45*, 4101–4115.
(3) Joo, S. H.; Choi, S. J.; Oh, I.; Kwak, J.; Liu, Z.; Terasaki, O.; Ryoo, R. *Nature* **2001**, *412*, 169–172.
(4) Yuasa, M.; Yamaguchi, A.; Itsuki, H.; Tanaka, K.; Yamamoto, M.; Oyaizu, K. *Chem. Mater.* **2005**, *17*, 4278–4281.
(5) Liu, Z.; Xing, Y.; Chen, C.; Zhao, L.; Suib, S. L. *Chem. Mater.* **2008**, *20*, 2069–2071.
(6) Shao, M.; Sasaki, K.; Adzic, R. R. *J. Am. Chem. Soc.* **2006**, *128*, 3526–3527.
(7) Fernandez, J. L.; Walsh, D. A.; Bard, A. J. *J. Am. Chem. Soc.* **2005**, *127*, 357–365.
(8) Savadogo, O.; Lee, K.; Oishi, K.; Mitsushimas, S.; Kamiya, N.; Ota, K. I. *Electrochem. Commun.* **2004**, *6*, 105–109.
(9) Sarkar, A.; Murugan, A. V.; Manthiram, A. *J. Phys. Chem. C* **2008**, *112*, 12037–12043.
(10) Adzic, R. R. Presented at DOE Hydrogen and Fuel Cell Review Meeting, Philadelphia, PA, 2004.
(11) Wang, X.; Kariuki, N.; Vaughey, J. T.; Goodpaster, J.; Kumar, R.; Myers, D. J. *J. Electrochem. Soc.* **2008**, *155*, B602.
(12) Kim, S. W.; Kim, M.; Lee, W. Y.; Hyeon, T. *J. Am. Chem. Soc.* **2002**, *124*, 7642–7643.
(13) Lim, B.; Xiong, Y. J.; Xia, Y. N. *Angew. Chem., Int. Ed.* **2007**, *46*, 9279–9282.
(14) Sun, Y. G.; Mayers, B. T.; Xia, Y. N. *Adv. Mater.* **2003**, *15*, 641–646.
(15) Xiong, Y. J.; Wiley, B. J.; Chen, J. Y.; Li, Z. Y.; Yin, Y. D.; Xia, Y. N. *Angew. Chem., Int. Ed.* **2005**, *44*, 7913–7917.
(16) Sun, Y. G.; Wiley, B.; Li, Z. Y.; Xia, Y. N. *J. Am. Chem. Soc.* **2004**, *126*, 9399–9406.

 Published on Web 06/29/2009 

substituting Ag nanoparticles with Co nanoparticles as templates.[17−20] However, to prepare metal nanoparticles, it is usually inevitable that organic reducing agent, surfactant and/or capping agent, and high temperature are involved.[13,21] Consequently, it is highly favorable to develop environmentally benign and effective fabrication route to hollow nanostructures with desired properties. While we have been studying a simple corrosion method to make functional porous metals,[22] recently we successfully fabricated nanoporous copper (NPC) by dealloying CuAl alloys. Realizing that NPC may work as an efficient and easily available template material, we speculate that a similar replacement reaction based on NPC may allow the construction of interesting three-dimensional metallic nanostructures with hollow interiors. Indeed, based on this concept, we have successfully fabricated PtCu bimetallic nanostructures that showed novel nanotubular mesoporous morphology and high activity toward methanol electrooxidation with enhanced CO tolerance.[23] In the current work, we describe the fabrication of nanotubular mesoporous PdCu (NM-PdCu) alloy structures with a nanoporous shell, with an emphasis on their electrocatalytic performance for important electrode reactions such as ORR. Intriguingly, the resulted PdCu nanostructures exhibit superior ORR activity than that of the commercial Pt/C catalyst, which suggests their great potential in fuel cells as highly efficient and cost-effective catalysts.

## Experimental Section

The $Cu_{25}Al_{75}$ (atom %) alloy foils were made by melting high-purity (99.9%) Cu and Al in an arc-furnace, followed by melt-spinning in $N_2$ atmosphere. NPC was prepared by etching CuAl alloy foils in 1.0 M NaOH for 5 h at 30 °C. The NPC samples were stored in $N_2$ saturated ultrapure water to avoid oxidation. In a typical replacement reaction, ~10 mg of freshly made NPC was quickly added into $K_2PdCl_4$ aqueous solution (1.2 mM, 150 mL) in a three-neck flask. The reaction was performed at 5 °C under $N_2$-protected magnetic stirring conditions for 150 min.

XRD data was recorded on a Bruker D8 advanced X-ray diffractometer using Cu Kα radiation ($\lambda$ = 1.5418 Å) at a step rate of 0.02°/s. UV−vis spectra were recorded on a Shimadzu UV-1700 spectrophotometer at room temperature. The morphological and compositional characterizations were carried out with a JEOL JSM-6700F field emission SEM, equipped with an Oxford INCA x-sight energy dispersive X-ray spectrometer (EDS). TEM images were obtained from a JEM-2100 high-resolution TEM (HRTEM) (200 kV).

Electrochemical measurements were performed with a CHI 760C electrochemical workstation using a conventional three-electrode cell with Pt foil as a counter electrode and mercury sulfate electrode (MSE) as the reference electrode. The ORR activity was measured by using a PAR model 636 rotating disk electrode system in an $O_2$-saturated 0.1 M $HClO_4$ solution. All potentials presented in the current manuscript are given with respect to the reversible hydrogen electrode (RHE). The catalyst suspension solution was prepared by sonicating 4.0 mg of PdCu sample, 2.0 mg of carbon powder, 200 $\mu$L of isopropanol, and 200 $\mu$L of Nafion solution (0.5 wt %), and then 8 $\mu$L of as-prepared catalyst suspension was dropped onto a 5 mm-diameter glassy carbon electrode which was prepolished to a mirror-finish with 0.05 $\mu$m alumina slurry and used as the working electrode. Prior to electrochemical measurements, the electrolytes were deoxygenated by bubbling $N_2$ for 30 min except for the ORR measurements. Considering that certain Cu components in the as-prepared PdCu catalysts may be unstable in electrolytic solutions, all the activity measurements were recorded after the working electrodes reached the steady-state by continuous potential cycling in 0.1 M $HClO_4$ solution before each ORR measurement, unless otherwise mentioned. The ORR activities of the commercial E-TEK Pt/C (20 wt % on carbon) and Johnson-Matthey Pd/C (20 wt % on carbon) catalysts were also measured for comparison.

## Results and Discussion

Recently, a simple dealloying method has been proved to be very effective in generating novel nanoporous metal materials.[24] For example, Hayes et al. have reported that NPC can be easily fabricated by electrochemically dealloying Cu/Mn in $H_2SO_4$.[25] In our work, we use traditional Raney's method to prepare NPC,[26] that is, dealloying Cu/Al alloy foils in NaOH solution at room temperature, which generates uniform three-dimensional nanoporous structures with bicontinuous pore channels and solid ligaments around 50 nm (Figure 1a,1b). The preparation of NPC is extremely simple and clean and can be easily scaled up, using the most common reagents (such as NaOH) in aqueous solution. EDS analysis confirms that the residual Al is less than 3 atom % in the resulted NPC structure. As the standard electrode potential between $[PdCl_4]^{2-}$/Pd (0.591 V vs SHE) is higher than that of $Cu^{2+}$/Cu (0.342 V vs SHE), a spontaneous galvanic replacement reaction will occur at mild temperature driven by the difference of the equilibrium electrode potentials. We know that templating Ag nanoparticles with a similar replacement reaction may result in interfering AgCl precipitates; therefore high temperature reflux or adding a little ammonia is a common strategy to avoid or eliminate this problem.[13] In contrast, the replacement reaction based on NPC can proceed much easier under mild conditions because Cu is relatively active and the yielded $CuCl_2$ salt is highly soluble.

Considering that the $[PdCl_4]^{2-}$ aqueous solution has characteristic absorption behavior, we used UV−vis absorption

(17) Liang, H. P.; Zhang, H. M.; Hu, J. S.; Guo, Y. G.; Wan, L. J.; Bai, C. L. *Angew. Chem., Int. Ed.* **2004**, *43*, 1540–1543.
(18) Liang, H. P.; Lawrence, N. S.; Wan, L. J.; Jiang, L.; Song, W. G.; Jones, T. G. J. *J. Phys. Chem. C* **2008**, *112*, 338–344.
(19) Zhang, J.; Qiu, C.; Ma, H.; Liu, X. *J. Phys. Chem. C* **2008**, *112*, 13970–13975.
(20) Ge, J.; Xing, W.; Xue, X.; Liu, C.; Lu, T.; Liao, J. *J. Phys. Chem. C* **2007**, *111*, 17305–17310.
(21) Chen, Z.; Waje, M.; Li, W.; Yan, Y. *Angew. Chem., Int. Ed.* **2007**, *46*, 4060–4063.
(22) Xu, C. X.; Su, J. X.; Xu, X. H.; Liu, P. P.; Zhao, H. J.; Tian, F.; Ding, Y. *J. Am. Chem. Soc.* **2007**, *129*, 42–43.
(23) Xu, C.; Wang, L.; Wang, R.; Wang, K.; Zhang, Y.; Tian, F.; Ding, Y. *Adv. Mater.* **2009**, *21*, 2165–2169.
(24) Erlebacher, J.; Aziz, M. J.; Karma, A.; Dimitrov, N.; Sieradzki, K. *Nature* **2001**, *410*, 450–453.
(25) Hayes, J. R.; Hodge, A. M.; Biener, J.; Hamza, A. V.; Sieradzki, K. *J. Mater. Res.* **2006**, *21*, 2611–2616.
(26) Raney, M. *Ind. Eng. Chem.* **1940**, *32*, 1199–1203.

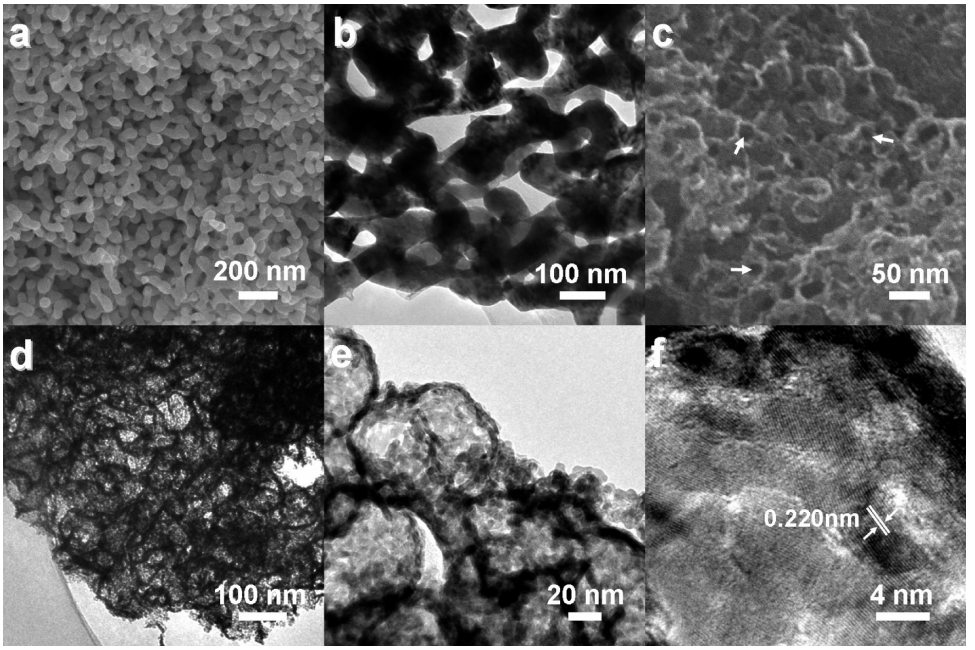


**Figure 1.** SEM and TEM (HRTEM) images of NPC (a, b) and nanotubular mesoporous PdCu bimetallic nanostructure (c−f), respectively.

spectra to monitor the reaction process momentarily. As shown in Figure 2a, upon mixing NPC with the $[PdCl_4]^{2-}$ aqueous solution, the absorption peak at ~210 nm decreases quickly in intensity, and after 150 min, the trend slows down, indicating a near complete conversion of NPC to a Pd-based nanostructure. By comparing these absorption curves with the calibrated standard plot (Figure 2c), we can estimate the amount of Cu replaced with Pd and the corresponding composition in the resulted structure during the entire reaction process (Figure 2b). For example, after reacting for 150 min, the content of Pd in the resulted nanostructure accounts for ~82 atom %, which is in excellent agreement with the EDS results which will be discussed below.

SEM observation shows that the resulted PdCu bimetallic nanostructure maintains very well the initial 3D porous structure of NPC template despite a slight increase of the ligament size from the original 50 nm to ~60 nm (Figure 1c). Some tubular openings can be clearly observed as marked with arrows, which also allows us to estimate the shell thickness to be less than 5 nm. The TEM image in Figure 1d demonstrates a clear contrast between dark edges and bright center portions from hollow ligaments, which have a tube diameter around 60 nm and shell thickness around 4 nm, indicating the formation of a nanotubular mesoporous nanostructure.[27] Higher magnification imaging allows closer inspection of the shell structure, and from Figure 1e, it is interesting to find that the shell surfaces are comprised of many small pores and grains around 3 nm rather than being smooth and seamless, suggesting the formation of a third order porosity at sub-5-nm scale. The structural details of these shells were further revealed by HRTEM (Figure 1f), from which one sees single crystalline bimetallic PdCu nanoparticles with size 3−4 nm interconnecting with each other to form a porous network. The lattice spacing of NM-PdCu in the HRTEM image was calculated to be ~0.220 nm, which corresponds to the (111) crystal plane of the PdCu alloy structure. By using the Brunauer−Emmett−Teller (BET) method, the surface area and pore size of NM-PdCu were measured to be ~32.4 $m^2\ g^{-1}$ and ~3.4 nm with a Quadrasorb SI-MP Surface Area (Quantachrome Instruments). As will be discussed below, this structural feature will be particularly advantageous to their electrocatalytic properties because the interconnecting metallic scaffold structure in all three dimensions allows excellent electron transport while the structure hollowness at higher length scale benefits the transport of targeted molecules (such as $O_2$) for surface reactions.

To gain insight into the structural formation and evolution, XRD was used to examine the crystal structures of samples during the reaction. As shown in Figure 3, after reacting for 60 min, the diffraction peaks from Cu are mostly suppressed. Meanwhile, three broad diffraction peaks located at around 42.0, 48.7, and 71.1 ($2\theta$) show up, which gradually shift to lower angle direction and increase in intensity as the reaction goes on. For the 150 min sample, the well-defined diffraction peaks sit well within the range of the expected diffractions for pure Pd and Cu, indicating the formation of a PdCu alloy structure. The asymmetric peaks with the tail at the higher-angle side suggest the formation of a Pd-rich overlayer[28] on the surface, which leads to the termination of replacement reaction due to the surface passivation. The composition analysis with EDS gives a nominal composition of $Pd_{85}Cu_{15}$ (atom %) for the 150 min sample, which is consistent with the estimated composition based on the quantitative UV−vis absorption data

(27) Ding, Y.; Mathur, A.; Chen, M. W.; Erlebacher, J. *Angew. Chem., Int. Ed.* **2005**, *44*, 4002–4006.

(28) Shao, M. H.; Huang, T.; Liu, P.; Zhang, J.; Sasaki, K.; Vukmirovic, M. B.; Adzic, R. R. *Langmuir* **2006**, *22*, 10409–10415.

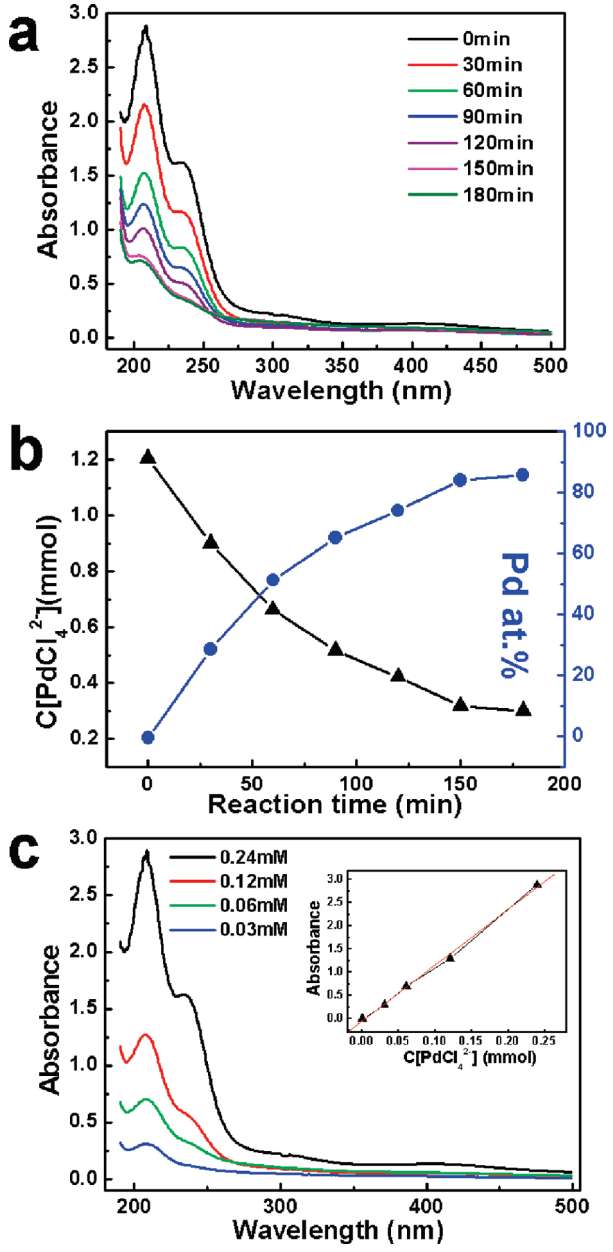


**Figure 2.** (a) UV−vis absorption spectra of the reaction solution at different reaction stages. (b) The quantification information at different reaction stages based on adsorption curves and the stoichiometry of the reaction: Cu + $[PdCl_4^{2-}] = Cu^{2+} + Pd + 4Cl^-$, assuming a 100% efficiency of the replacement reaction. The left (black) and right (blue) axes represent the concentration of $[PdCl_4^{2-}]$ and the Pd ratio in the resulted PdCu bimetallic nanostructure, respectively, at a specific reaction time. (c) UV−vis absorbance spectra of the standard $K_2PdCl_4$ solutions. The corresponding linear correlation between $K_2PdCl_4$ concentration and absorbance intensity is shown as an inset in (c).

(Figure 2). It is quite interesting that although the reaction proceeds at below room temperature, the interdiffusion between Cu and the deposited Pd atoms is so quick that a gradient-structured PdCu alloy can form within minutes after the initiation of the reaction. This observation is actually not unexpected because low temperature alloying has been frequently observed from bimetallic nanoparticles.[29] Ghodbane[30] et al. have investigated the mechanism of exchange reaction between Pd-containing solution and Cu electrode and found that the oxidation of Cu by the existing oxygen dissolved in solution was involved besides the replacement reaction between Cu and palladium ions. In contrast, the use of $N_2$ in our reaction can effectively prevent the oxidation of NPC. The appearance of a little $Cu_2O$ (marked with an asterisk) should be ascribed to the oxidation of the exposed Cu during the drying process.

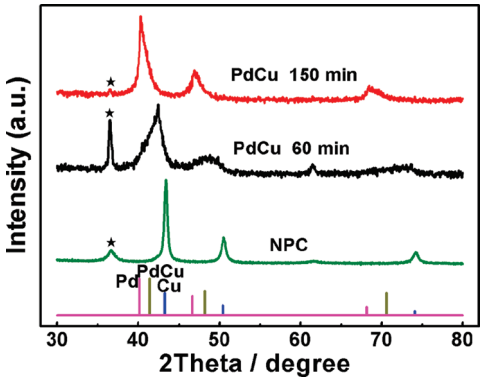


**Figure 3.** XRD patterns for NPC and the resulted bimetallic PdCu samples at different reaction stages (60 and 150 min). The standard patterns for pure Pd (JCPDS 65-2867), Cu (JCPDS 04-0836), and PdCu alloy (JCPDS 48-1551) are attached at the bottom for comparison. A little $Cu_2O$ (marked as ∗) was found in some samples because of the partial oxidation of the exposed Cu on sample surfaces.

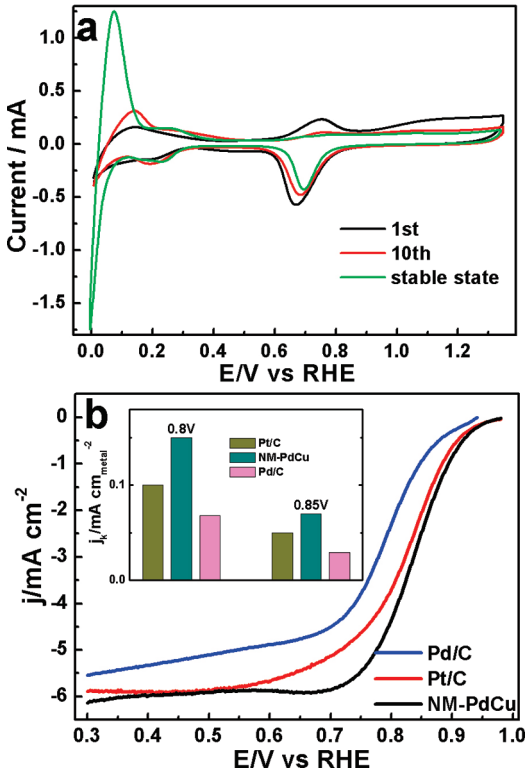


**Figure 4.** (a) Cyclic voltametric curves (CVs) of NM-PdCu sample in 0.1 M $HClO_4$ solution. Scan rate: 20 mV $s^{-1}$. (b) Polarization curves for the ORR on NM-PdCu and Pd/C, Pt/C nanoparticles in an $O_2$-saturated 0.1 M $HClO_4$ at room temperature at 1600 rpm. Scan rate: 5 mV $s^{-1}$. Inset is the specific activity for NM-PdCu, Pt/C, and Pd/C catalysts at 0.8 and 0.85 V, respectively.

(29) Shibata, T.; Bunker, B. A.; Zhang, Z. Y.; Meisel, D.; Vardeman, C. F.; Gezelter, J. D. *J. Am. Chem. Soc.* **2002**, *124*, 11989–11996.
(30) Ghodbane, O.; Roué, L.; Bélanger, D. *Chem. Mater.* **2008**, *20*, 3495–3504.

The hollow structure makes NM-PdCu an ideal electrode material for electrocatalytic applications. Pd-based nanostructures have shown extraordinary activity toward many important reactions such as CO oxidation, formic acid electrooxidation, ORR, and so forth.[31−35] Herein, we focus on their performance in ORR reactions in view of their potential as cathode catalysts for PEMFC application. Cyclic voltammetry was first used to probe its surface state. Figure 4a presents the voltammetric behavior of NM-PdCu sample in 0.1 M $HClO_4$ solution. During the first scan, the anodic peak at 0.6−0.85 V can be attributed to the leaching of exposed Cu atoms from the surface layer. In the subsequent scans, the hydrogen region (0−0.3 V) gradually evolves into a well-defined voltammetric profile of hydrogen absorption/desorption and hydrogen evolution. Meanwhile, the reduction peak for palladium oxide shifts slightly toward the positive potential direction and eventually stabilizes at ~0.70 V. The disappearance of the Cu dissolution peak suggests the formation of nearly pure Pd-skin on the catalyst surface. Figure 4b shows the ORR polarization curves for NM-PdCu, Pd/C, and Pt/C catalysts in $O_2$-saturated 0.1 M $HClO_4$ solution. Clearly, NM-PdCu catalyst exhibits a half-wave potential of 0.840 V for the ORR, which is nearly 60 mV more positive as compared with that of the commercial Pd/C catalyst (0.78 V), indicating a greatly enhanced ORR activity. Intriguingly, the NM-PdCu catalyst is also superior to the commercial Pt/C (0.825 V) catalyst with more positive half-wave potential. The inset in Figure 4b shows that NM-PdCu has the highest specific activity at 0.8 and 0.85 V among three catalysts, which is 1.5 and 1.4 times of the activity of Pt/C catalyst at the respective potential. The real surface area of Pd for the used electrode catalysts was estimated by integrating the amount of reduction charge corresponding to the surface oxide stripping reaction in 1 M $H_2SO_4$ solution from 0 to 1.35 V at 50 mV/s.[36] Recent studies have demonstrated that Pd catalysts can produce high ORR activity when combined with appropriate transition metals such as Co, Fe, Mo, and so forth.[6,7,9,37] Here, our results clearly demonstrate that the ORR activity of Pd can also be greatly enhanced by alloying with Cu. It is well-known that Pt catalysts are usually significantly better than Pd catalysts in view of their ORR activities (Figure 4b). However, here we achieved even better activity than that of Pt, merely because we have added a common non-noble metal such as Cu into the Pd lattices.

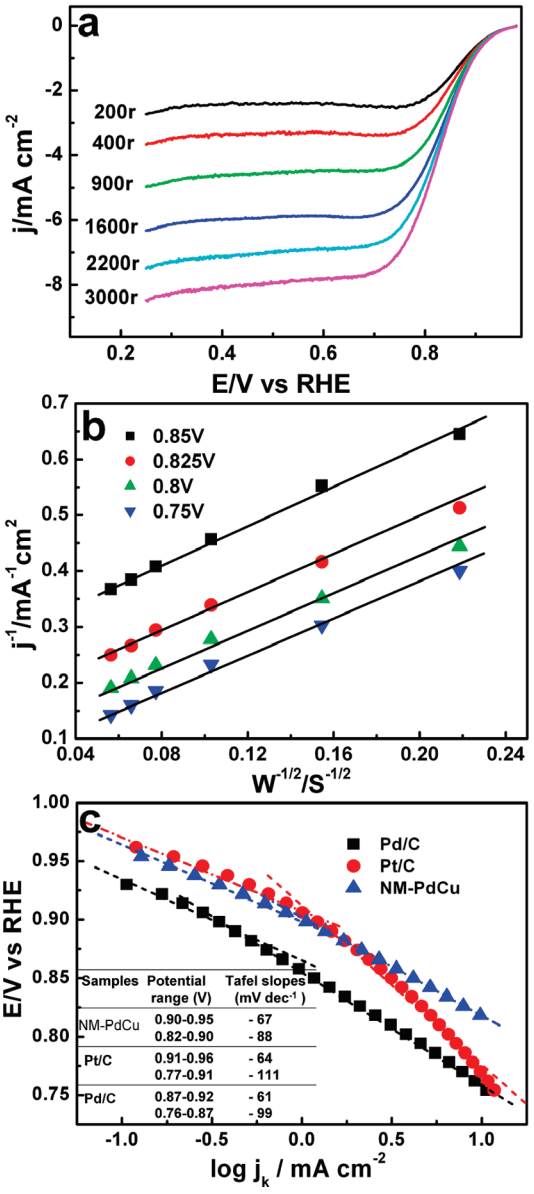


**Figure 5.** (a) Polarization curves of ORR on NM-PdCu catalyst in an $O_2$-saturated 0.1 M $HClO_4$ solutions at different rotation rates. (b) The corresponding Koutecky−Levich plots at different potentials. (c) Tafel plots of ORR on NM-PdCu, Pt/C, and Pd/C catalysts at 1600 rpm. Inset shows the corresponding Tafel slopes.

This is of considerable importance for their application as the cathode electrocatalysts for the ORR.

Figure 5a profiles a group of polarization curves for the ORR on the NM-PdCu catalyst at different rotation rates at room temperature. Figure 5b shows the corresponding Koutecky−Levich plots obtained from the inverse current density ($j^{-1}$) as a function of the inverse of the square root of the rotation rate ($\omega^{-1/2}$). The good linearity and parallelism of these plots indicate the first-order kinetics with respect to molecular oxygen. From the slope of the Koutecky−Levich plot, the so-called B factor was estimated to be 0.084 mA $rpm^{-1/2}$. According to equation $B = 0.62nFAD^{2/3}\nu^{-1/6}C_{O_2}$ ($n = 4$), the corresponding value is calculated to be 0.08 mA $rpm^{-1/2}$ by imputing the values for the Faraday constant $F$, the electrode's geometric area $A$, and the reported parameters for oxygen solubility,

(31) Wilson, O. M.; Knecht, M. R.; Garcia-Martinez, J. C.; Crooks, R. M *J. Am. Chem. Soc.* **2006**, *128*, 4510–4511.
(32) Solsona, B. E.; Edwards, J. K.; Landon, P.; Carley, A. F.; Herzing, A.; Kiely, C. J.; Hutchings, G. J. *Chem. Mater.* **2006**, *18*, 2689–2695.
(33) Gallon, B. J.; Kojima, R. W.; Kaner, R. B.; Diaconescu, P. L. *Angew. Chem., Int. Ed.* **2007**, *46*, 7251–7254.
(34) Yu, J.; Ding, Y.; Xu, C.; Inoue, A.; Sakurai, T.; Chen, M. *Chem. Mater.* **2008**, *20*, 4548–4550.
(35) Xiao, L.; Zhuang, L.; Liu, Y.; Lu, J.; Abruña, H. D. *J. Am. Chem. Soc.* **2009**, *131*, 602–608.
(36) Pan, W.; Zhang, X.; Ma, H.; Zhang, J. *J. Phys. Chem. C* **2008**, *112*, 2456–2461.
(37) Raghuveer, V.; Manthiram, A.; Bard, A. J. *J. Phys. Chem. B* **2005**, *109*, 22909–22912.

$C_{O_2}$ ($C_{O_2} = 1.26 \times 10^{-3}$ mol $L^{-1}$), oxygen diffusivity, $D$ ($D = 1.93 \times 10^{-5}$ $cm^2$ $s^{-1}$), and kinetic viscosity of the electrolyte, $\nu$ ($\nu = 1.009 \times 10^{-2}$ $cm^2$ $s^{-1}$).[38,39] The good accordance between the experimental and theoretical $B$ value indicates a nearly complete reduction of $O_2$ to $H_2O$ on the NM-PdCu surface via a four-electron reaction process.

The Tafel plots for the NM-PdCu catalyst are shown in Figure 5c along with those of Pt/C and Pd/C catalysts included for comparison by using the Koutecky−Levich method. The obtained plots for all catalysts can be fitted by two linear segments. The Tafel parameters corresponding to each catalyst are shown in the inset in Figure 5c. For NM-PdCu, one slope is estimated to be −67 mV $dec^{-1}$ in the potential range of 0.90−0.95 V, while the others are −88 mV $dec^{-1}$ in the lower potential range, respectively. The two Tafel slopes for Pd/C catalyst are 61 and 99 mV $dec^{-1}$ in the high- and low-potential range, respectively, whereas Pt/C catalyst shows the corresponding Tafel slopes at −64 and −111 mV $dec^{-1}$, indicating different ORR behaviors within different potential ranges. The exchange current density corresponding to each Tafel slope of NM-PdCu, Pt/C, and Pd/C catalysts was calculated to be $1.6 \times 10^{-5}$, $1.0 \times 10^{-5}$, and $7.94 \times 10^{-6}$ mA $cm^{-2}$ by extrapolating the potential from the higher potential range to the reversible oxygen electrode potential,[40] implying a higher ORR activity on NM-PdCu. Adzic and co-workers have also found two Tafel slopes of −81 and −96 mV $dec^{-1}$ in the similar potential range on Pd/Pt(111) in 0.1 M $HClO_4$ solution.[28] They have evaluated an intrinsic Tafel slope of −118 mV $dec^{-1}$ in acidic solutions in the absence of adsorbed anions.[41] The slight deviation of the Tafel slopes for NM-PdCu catalyst may be related to a variation of adsorbed oxygen-containing species on catalyst surface in the potential range studied.[38,39]

It is known that the PEMFCs' efficiency will dramatically degrade when the methanol permeates to the cathode side because Pt-containing catalysts usually have very little methanol tolerance.[42] Consequently, it is of practical importance for the cathode catalyst to possess high methanol tolerance for application in PEMFCs. We detected the ORR activity of NM-PdCu catalyst in the presence of methanol by using RDE measurement. As shown in Figure 6a, the half-wave potential only undergoes a slight negative shift of ~40 mV in the mixed solution of 0.1 M $HClO_4$ + 0.1 M $CH_3OH$, indicating a respectable ORR activity even in the presence of methanol. To explore the possible origination for the small decrease of ORR activity, the electrocatalytic behavior of NM-PdCu catalyst toward methanol oxidation was

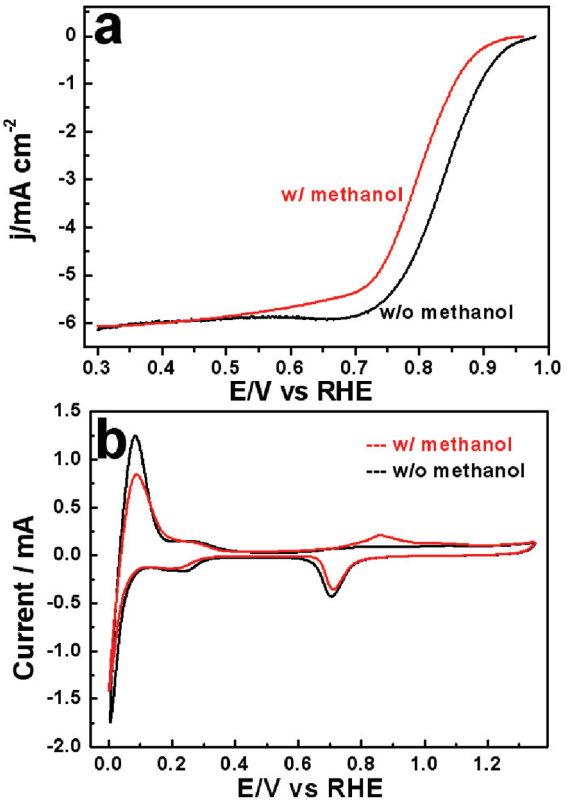


**Figure 6.** (a) Polarization curves for the ORR on NM-PdCu catalyst in an oxygen-saturated 0.1 M $HClO_4$ solution with (w/, red) and without (w/o, black) 0.1 M methanol at a rotation rate of 1600 rpm; scan rate: 5 mV $s^{-1}$. (b) CV curves of NM-PdCu catalyst in an $N_2$-purged 0.1 M $HClO_4$ solution with (red) and without (black) 0.1 M methanol; scan rate: 20 mV $s^{-1}$.

examined by cyclic voltammetry. From Figure 6b, it can be found that in the presence of methanol both the hydrogen region and palladium reduction peak for NM-PdCu slightly reduce in intensity. Moreover, a small peak emerges at ~0.7 V was found to superimpose onto the onset potential for Pd oxidation as compared with that in methanol-free solution. This anodic peak should be ascribed to the weak oxidation of methanol molecules on oxidized Pd surfaces. Accordingly, the adsorption of methanol and/or the related partially oxidized intermediates on NM-PdCu surface possibly causes the decrease of ORR activity in the presence of methanol as described above.

On the basis of the experimental observations, NM-PdCu bimetallic catalyst shows excellent ORR activity with enhanced methanol tolerance as compared with the commercial Pt/C and Pd/C catalysts. This performance improvement is obviously related to the special structure configuration of our catalyst. During the voltammetric measurements, Cu atoms on the surface are progressively dissolved, and accordingly, the neighboring Pd atoms will undergo a reconstruction at the NPC/electrolyte interface to form a unique PdCu alloy structure with a nearly pure Pd-skin, and the residual Cu atoms are buried within the subsurface atomic layers.[43] These sublayer Cu atoms may

(38) Stamenković, V.; Schmidt, T. J.; Ross, P. N.; Marković, N. M. *J. Phys. Chem. B* **2002**, *106*, 11970–11979.
(39) Zhang, J.; Mo, Y.; Vukmirovic, M. B.; Klie, R.; Sasaki, K.; Adzic, R. R. *J. Phys. Chem. B* **2004**, *108*, 10955–10964.
(40) Gonzalez-Huertal, R. G.; Pierna, A. R.; Solorza-Feria, O. *J. New Mat. Electrochem. Systems* **2008**, *11*, 63–67.
(41) Wang, J. X.; Markovic, N. M.; Adzic, R. R. *J. Phys. Chem. B* **2004**, *108*, 4127–4033.
(42) Li, H. Q.; Xin, Q.; Li, W. Z.; Zhou, Z. H.; Jiang, L. H.; Yang, S. H.; Sun, G. Q. *Chem. Commun.* **2004**, 2776–2777.
(43) Knudsen, J.; Nilekar, A. U.; Vang, R. T.; Schnadt, J.; Kunkes, E. L.; Dumesic, J. A.; Mavrikakis, M.; Besenbacher, F. *J. Am. Chem. Soc.* **2007**, *129*, 6485–6490.

provide an electronic modification for the topmost Pd layer by a surface strain effect or an alloying effect,[44,45] which may provide unique surface sites for the adsorption of $O_2$ molecules and be beneficial for their subsequent electro-reduction.[7,46] Recently, Koh et al. reported that dealloyed Pt-rich Pt−Cu catalyst could exhibit enhanced ORR activity, which was ascribed to a strained Pt surface structure due to the interaction of the low concentration of near-surface Cu atoms with surface Pt atoms.[47] Furthermore, the three-dimensional bicontinuous spongy structure and various hollow channels provide good transport channels for medium molecules and electrons, which may greatly facilitate the reaction kinetics of ORR on the catalyst surfaces. Further studies are still needed to establish an explicit picture for the enhanced ORR activity as well as a physical correlation between structures and properties in this novel high surface area, bimetallic nanocatalyst system.

## Conclusions

We have demonstrated a simple approach to the fabrication of novel nanotubular mesoporous PdCu bimetallic catalyst with a nanoporous shell based on a low temperature dealloying in aqueous solution and a subsequent in situ galvanic replacement reaction. By using NPC as both a template and reducing agent, the replacement reaction can be easily performed at room temperature because Cu is more active and the resulted $CuCl_2$ salt is soluble. Interestingly, the resulted NM-PdCu catalyst exhibits a superior ORR activity as compared to commercial Pt/C and Pd/C catalyst. It is suggested that the trimodal hollow bimetallic structure in NM-PdCu plays crucial roles for the enhancement of ORR activity. With obvious advantages of unique catalytic activities, low cost, and simple processing, our method can be easily extended to make a wide variety of nanotubular mesoporous bimetallic composites, using various metal templates and catalytically active metal precursors. Being compatible with the current processing techniques for actual device applications, these novel nanomaterials see great potential for use in heterogeneous catalysis and energy-related fields such as fuel cells.

**Acknowledgment.** This work was supported by the National 863 (2006AA03Z222) and 973 (2007CB936602) Program Projects of China, the Key Project of Chinese Ministry of Education (108078), and the Natural Science Foundation of Shandong Province (Y2007B33). Y.D. is a Tai-Shan Scholar supported by the SEM-NCET, SRF-ROCS Programs and the Shandong Natural Science Fund for Distinguished Young Scholars.

(44) Abel, M.; Robach, Y.; Porte, L. *Surf. Sci.* **2002**, *498*, 244–256.
(45) Nilekar, A. U.; Xu, Y.; Zhang, J.; Vukmirovic, M. B.; Sasaki, K.; Adzic, R. R.; Mavrikakis, M. *Top. Catal.* **2007**, *46*, 276–284.
(46) Stamenkovic, V. R.; Mun, B. S.; K.; Mayrhofer, J. J.; Ross, P. N.; Markovic, N. M. *J. Am. Chem. Soc.* **2006**, *128*, 8813–8819.
(47) Koh, S.; Strasser, P. *J. Am. Chem. Soc.* **2007**, *129*, 12624–12625.